Research Article

Development of Kimpul Starch-Based Composite Films Reinforced with TEMPO-Oxidized Cellulose Microfiber for Food Packaging

Fadlan Hidayat*
Department of Agricultural Industrial Engineering, Faculty of Agricultural Technology, Universitas Serambi Mekkah, Banda Aceh, Indonesia

Anita Noviyanti
Department of Biology Education, Faculty of Teacher Training and Education Universitas Serambi Mekkah, Banda Aceh, Indonesia

Rahmi
Department of Chemistry, Faculty of Mathematics and Natural Sciences, Universitas Syiah Kuala, Banda Aceh, Indonesia

Eti Indarti
Department of Agricultural Product Technology, Faculty of Agriculture, Universitas Syiah Kuala, Banda Aceh, Indonesia

Salfauqi Nurman
Department of Marine Engineering, Politeknik Pelayaran Malahayati, Aceh Besar, Indonesia

Andriy Anta Kacaribu
Doctoral Program of Agricultural Science, Postgraduate School, Universitas Syiah Kuala, Banda Aceh, Indonesia

* Corresponding author. E-mail: fadlanhidayat@serambimekkah.ac.id DOI: 10.14416/j.asep.2026.04.001
Received: 18 November 2025; Revised: 10 December 2025; Accepted: 26 January 2026; Published online: 2 April 2026

Abstract
This study investigated the development of starch-based films reinforced with TEMPO-oxidized cellulose microfibrils (TOCMF) using kimpul starch as the primary polymer matrix. A Box Behnken Design (BBD) combined with Response Surface Methodology (RSM) was employed to evaluate the effects of starch, TOCMF, and glycerol contents on the mechanical properties (tensile strength (TS) and elongation at break (EAB)). The quadratic models were statistically significant with high coefficients of determination (R^2 = 0.86–0.98) and non-significant lack-of-fit, confirming their adequacy for prediction and optimization. The optimized film formulation achieved superior mechanical properties, with TS (38.78 MPa) higher than most previously reported starch-based films, while maintaining desirable flexibility (EAB = 18.59%). This work highlights the potential of underutilized kimpul starch incorporated with TOCMF to develop packaging films with superior functional performance, providing new insights into the design of sustainable materials for food packaging applications. Moreover, the use of kimpul, a low-cost and locally abundant tuber, offers an additional advantage by promoting value-added utilization of indigenous resources for environmentally friendly packaging.

Keywords: Biodegradable films, Food packaging, Kimpul starch, Polymer composites, TEMPO-oxidized cellulose microfibers

1 Introduction

The excessive use of petroleum–based plastics for food packaging poses significant environmental challenges due to their persistence and the resulting microplastic pollution [1]. In response to regulatory requirements and global concern, biodegradable options derived from renewable resources are gaining attention [2]. Polysaccharide–based biopolymers, such as chitosan, cellulose, and polylactic acid (PLA, derived from lactic acid), have been extensively investigated as sustainable alternatives to conventional plastics in food packaging applications due to their biodegradability, biocompatibility, and safety for food contact [3]–[7]. Despite these advantages, achieving desirable film properties often requires costly processing or complex modifications, which may limit their large–scale application [8]. In contrast, starch is considered a top candidate, valued for its wide availability, low cost, inherent biodegradability, and excellent film–forming ability [9].

However, their practical application remains limited due to inherent drawbacks, including poor mechanical strength, brittleness, and high moisture sensitivity [9], [10]. These shortcomings significantly reduce their effectiveness, particularly under humid conditions, thereby restricting their use in food packaging. Most studies have reinforced starch matrices with fillers to overcome these limitations and enhance structural integrity and barrier properties [11], [12]. Among these, cellulose nanofibers (CNFs) and microfibers (CMFs), particularly those prepared via TEMPO–mediated oxidation, are of great interest due to their high aspect ratio, high mechanical strength, and abundant carboxyl groups that can form strong interactions with starch chains [13]. Incorporation of CMF has been shown to markedly improve the tensile strength, water resistance, and barrier properties of starch–based films [14], [15].

Despite these advances, research has predominantly focused on conventional starches such as corn, cassava, maize, wheat, rice, and potato [16], [17]. In contrast, studies on underutilized tropical tubers such as kimpul (*Xanthosoma sagittifolium*), widely cultivated in tropical regions and rich in amylopectin with promising film–forming potential [18], remain limited. Broadening the range of starch resources diversifies material options, promotes the utilization of local biodiversity, and adds value to tropical tubers by fostering their industrial application in eco–friendly packaging, thereby supporting both environmental sustainability and regional economies.

Several studies have demonstrated the reinforcing effect of cellulose fillers in starch–based films. Sasria *et al*., reported that combining jackfruit seed starch with cellulose from oil palm empty fruit bunches (OPEFB) and carboxymethyl cellulose (CMC) achieved a maximum tensile strength of 5.44 MPa, depending on plasticizer content [19]. Abdullah *et al*., incorporated microcrystalline cellulose (MCC) into cassava starch films, significantly increasing tensile strength to 16.7 MPa at 20% filler loading, although elongation at break decreased markedly [20]. Likewise, Saputri *et al*., [21] used cellulose derived from banana bunch fibers to reinforce cassava starch, resulting in an increase in tensile strength from 2.92 MPa to 6.72 MPa and reduced water vapor absorption at an optimal filler content of 7.5%. These findings confirm the role of cellulose as an effective reinforcement in starch matrices; nevertheless, they mainly rely on conventional starch sources and commonly use MCC or untreated natural fibers, which often exhibit limited interfacial compatibility with starch.

Moreover, although the mechanical properties of these films were enhanced, the tensile strength values obtained remain relatively modest for high–performance food packaging applications. To date, no attention has been given to the use of non–traditional starches such as kimpul, which possesses high amylopectin content and promising film–forming ability. At the same time, TEMPO–oxidized cellulose microfibers (TOCMF) offer stronger bonding potential [22], but have rarely been integrated into starch-based packaging films. Notably, nata de coco represents a highly sustainable, low–cost, and abundant cellulose source for producing TOCMF. Nata de coco is microbially synthesized, requires minimal land resources, and uses simple agricultural by-products as feedstock, making it an eco–friendly and renewable cellulose source compared to plant–derived cellulose that requires intensive pretreatment and generates chemical waste [23]. The use of nata de coco as a TOCMF precursor introduces a novel and sustainable strategy for biopolymer reinforcement.

Therefore, integrating kimpul starch with TOCMF derived from nata de coco offers a novel strategy to overcome the mechanical and barrier limitations of starch–based films. The aims of the present study: (i) the use of an underutilized tropical starch with high amylopectin content, and (ii) the

valorization of nata de coco as a sustainable, microbially derived cellulose source for high–performance TOCMF. This study develops and characterizes kimpul starch–based composite films reinforced with TOCMF, systematically evaluating their mechanical, barrier, and thermal properties. The findings are expected to provide new insights into the utilization of underutilized tropical starches and cost–effective cellulose reinforcements as eco–friendly, high–performance materials for sustainable food packaging.

2 Materials and Methods

2.1 *Materials and equipment*

Nata de coco (Kara Brand) was purchased from a local market in Banda Aceh, Indonesia. Sodium chlorite ($NaClO_2$), sodium hydroxide (NaOH), and acetic acid (CH_3COOH) of analytical grade were supplied by Merck (Malaysia). TEMPO (2,2,6,6–tetramethylpiperidine–1–oxyl radical), sodium bromide (NaBr), sodium hypochlorite (NaClO), and ethanol were obtained from Sigma–Aldrich (Singapore). The equipment used included a household blender, ultrasonic bath (Bransonic 1510E), magnetic stirrer (HS–300), centrifuge (Hettich Zentrifugen EBA–20), analytical balance (Shimadzu AW220), pH meter (WTW ProfiLine–3110), and Whatman filter paper (125 mm).

2.2 *Preparation of CMF*

Cellulose microfibers (CMF) were prepared from nata de coco via TEMPO–mediated oxidation, adapted from a previously reported procedure [24] with specific modifications. Briefly, nata de coco was boiled and repeatedly washed to remove residual acetic acid bacteria. The material was then treated with 0.1 M NaOH and washed with distilled water until the pH was neutral. The alkali–treated cellulose was crushed to reduce particle size and subsequently purified in 0.1 M NaOH at 80 °C for 20 min, followed by thorough washing to obtain purified cellulose fibers.

For TEMPO oxidation, the purified cellulose (150 g, wet basis) was dispersed in distilled water containing TEMPO (0.115 mmol/g cellulose) and sodium bromide (0.617 mmol/g cellulose). The mixture was stirred in an ice–assisted ultrasonic bath to maintain the reaction temperature at approximately 25 °C. The pH was maintained at 10 for 4 h while the sodium hypochlorite solution was slowly added dropwise. After the oxidation reaction was completed, ethanol was added to terminate the reaction, and the suspension was washed repeatedly with distilled water.

Unlike the original protocol—which included post–oxidation using sodium chlorite and subsequent high–energy mechanical treatments such as ultrasonication or high–speed centrifugation to produce cellulose nanocrystals (CNC)—this study intentionally omitted all post-oxidation and mechanical disintegration steps. This modification was made to reduce energy consumption, minimize chemical use, and maintain a more straightforward, more sustainable process. As a result, the material obtained was TEMPO-oxidized cellulose microfibers (TOCMF) rather than nanoscale cellulose. The absence of post–oxidation preserves the microfiber–scale dimensions while introducing carboxyl functional groups on the cellulose surface, thereby enabling effective interaction with starch without requiring nanocellulose production. The resulting TOCMF was characterized using SEM, and particle size distribution was analyzed using ImageJ and OriginLab Pro (version 25). Other physicochemical characterizations of TOCMF have been reported in our previous publication [24].

2.3 *Preparation of composite films*

Composite films were fabricated based on the procedure of [24] with minor modifications. Kimpul starch was weighed according to the experimental formulation and dispersed in 150 mL of distilled water. The starch suspension was stirred at 60 rpm and heated on a hot plate at 90 °C for 20 min to achieve complete gelatinization. Glycerol and CMF were then incorporated as specified in the formulation, followed by continuous stirring for an additional 10 min under the same conditions to ensure uniform dispersion. The film–forming solution was cast into a 20 cm × 20 cm glass mold and leveled to obtain a consistent thickness. Drying was carried out in a hot–air oven at 60 °C for 24 h. The dried films were carefully peeled from the molds and subsequently conditioned in a desiccator prior to further characterization.

2.4 *Experimental design*

Response Surface Methodology (RSM) was used to design and analyze the experimental trials with the aid of Design–Expert software (Version 12, Stat–Ease Inc., Minneapolis, USA). A Box–Behnken Design (BBD) was selected, involving three independent variables, in order to evaluate factor interactions and determine the optimum film formulation. The independent variables were the concentrations of kimpul starch (A), TOCMF (B), and glycerol (C), as listed in Table 1 [24]. The number of runs required for the design was calculated according to the BBD model equation. The relationship between the independent variables and the responses was described by a second–order polynomial equation (Equation 1).

$$Y = \beta_0 + \beta_1 A + \beta_2 B + \beta_3 C + \beta_{12} AB + \beta_{13} AC + \beta_{23} BC + \beta_{11} A^2 + \beta_{22} B^2 + \beta_{33} C^2 + \varepsilon \quad (1)$$

where Y is the predicted response; β_0 is the intercept; β_1, β_2, β_3 are the linear coefficients; β_{12}, β_{13}, β_{23} are the interaction coefficients; β_{11}, β_{22}, β_{33} are the quadratic coefficients; A, B, C are the independent variables; and ε is the experimental error. The quadratic and interaction terms (A^2, B^2, C^2, AB, AC, BC) account for curvature and synergistic effects between formulation components.

Table 1: Experimental design of preparation of composite.

Independent variables	Unit	Level		
		-1	0	+1
Kimpul starch	%	5	5.5	6
TOCMF	%	1	1.25	1.5
Glycerol	%	2	2.5	3

TOCMF–TEMPO-oxidized cellulose microfibril.

2.5 *Characterizations*

Mechanical properties of the composite films were evaluated in accordance with ASTM D882–18 at a crosshead speed of 50 mm/min. Film specimens were cut into rectangular strips with a fixed width of 0.5 mm, and the thickness was measured at three points using a digital micrometer; the mean ± standard deviation is reported. The average film thickness across all formulations ranged from 0.083 to 0.267 mm. Tensile tests were performed using a gauge length of 50 mm. For each formulation, three replicate specimens were tested to obtain the tensile strength (TS) and elongation at break (EAB), which were calculated using Equations (2) and (3):

$$TS\ (MPa) = \frac{F_{max}}{A} \quad (2)$$

$$EAB\ (\%) = \frac{L_f - L_0}{L_0} \times 100 \quad (3)$$

where F_{max} is the maximum force applied to the specimen before breaking (N), A is the initial cross–sectional area of the film (mm^2), L_f is the film length at breaking point (mm), and L_0 is the initial film length (mm).

Two or three types of samples were subjected to further characterization: (i) neat starch film (control), (ii) starch–glycerol films, and (iii) starch–TOCMF–glycerol composite films with optimal mechanical properties obtained from RSM optimization. Functional group analysis was carried out using Fourier Transform Infrared Spectroscopy (FTIR, FTIR–650, Tianjin Gangdong Technology Development Co., Ltd., China) in the range of 4000–500 cm^{-1}. Crystallinity was determined by X–ray Diffraction (XRD), with scans performed in the 2θ range of 10–80°. The crystallinity index (CrI) was calculated using Origin software based on the method described in Segal *et al*. [25]. Morphological features of the films were observed using Scanning Electron Microscopy (SEM, JEOL JSM 6390 LA) operated at an accelerating voltage of 10–15 kV. Thermal stabilities assessed by Thermogravimetric Analysis (TGA), derivative thermogravimetric (DTG), and differential thermal analysis (DTA), where samples were heated from 0 to 500 °C at a heating rate of 10 °C/min under a nitrogen atmosphere.

2.6 *Composite film evaluations*

The swelling power (SP) of the films was measured by immersing the samples (2 × 2 cm) in distilled water at 25–27 °C for 2 h. For SP, duplicate evaluation was performed, data reported as mean ± SD. The weight loss (WL%) and mass retention (MR%) of grapes were evaluated after 7 days of storage. For the packaging test, grapes were wrapped using the optimized starch–TOCMF–glycerol composite film and the control starch–glycerol film. The samples were stored under typical ambient tropical conditions, with room temperature maintained at 25–28 °C and natural relative humidity estimated at 70–85%. Grapes were placed in sterile plastic containers that remained

open during storage to allow unrestricted airflow and simulate real household storage conditions without controlled ventilation. SP, WL%, and MR% were calculated using Equations (4)–(6):

$$SP\ (\%) = \frac{W_t - W_i}{W_i} \times 100 \quad (4)$$

$$WL\ (\%) = \frac{W_0 - W_7}{W_0} \times 100 \quad (5)$$

$$MR\ (\%) = 100 - WL\ (\%) \quad (6)$$

where W_i is the initial dry weight of the film (g), and W_t is the weight of the composite film after immersion (g). W_0 is the initial weight of the grape (g) and W_7 is the final weight of the grape after 7 days of storage (g).

3 Result and Discussions

3.1 *Response surface analysis*

Seventeen experimental runs were generated according to the central composite design (CCD), and the corresponding results for TS and EAB are summarized in Table 2. The mechanical responses varied considerably depending on the formulation. The analysis of variance (ANOVA) confirmed that the quadratic models for TS and EAB were significant (Table 3). The high coefficients of determination (R^2 = 0.9832 for TS, and 0.8608 for EAB indicated good agreement between the experimental and predicted values, suggesting that the proposed models can accurately describe the relationships between the independent variables and the mechanical responses. The non-significant lack–of–fit values for all three responses further validated the adequacy of the models, ensuring their suitability for optimization within the experimental design space.

The model for TS exhibited an F–value of 45.63 with a probability value of <0.0001, confirming the significance of the regression. Significant terms included the main effects of starch (A) and CMF (B), as well as their interactions (AB, AC, BC) and the quadratic effect of CMF (B^2). As illustrated in the 3D response surface plots (Figure 1(A)), TS increased markedly with increasing starch and CMF concentrations, reaching the maximum experimental value of 38.78 MPa under the combination of 5.5% starch, 1.5% CMF, and 2.0% glycerol (run 4, Table 2). The positive effect of CMF incorporation can be attributed to strong hydrogen bonding and efficient stress transfer between the TOCMF network and starch chains, which markedly improved film rigidity and strength. However, excessive glycerol addition resulted in a decline in TS due to its plasticizing effect, which disrupts polymer–polymer interactions and reduces cohesion.

Table 2: Experimental design result.

Run	S (%)	CMF (%)	Gly (%)	Response	
				TS (MPa)	EAB (%)
1	6.00	1.50	2.50	38.77	17.44
2	6.00	1.25	3.00	27.37	13.33
3	5.50	1.00	2.00	15.60	19.56
4	5.50	1.50	2.00	38.78	18.59
5	5.00	1.25	2.00	25.82	14.64
6	6.00	1.25	2.00	23.18	15.48
7	5.50	1.25	2.50	23.22	16.78
8	5.50	1.00	3.00	18.78	21.78
9	6.00	1.00	2.50	18.58	20.78
10	5.50	1.25	2.50	23.22	18.78
11	5.50	1.25	2.50	23.22	17.78
12	5.00	1.00	2.50	19.45	18.13
13	5.50	1.25	2.50	25.22	18.67
14	5.50	1.50	3.00	33.43	17.67
15	5.00	1.50	2.50	30.75	17.05
16	5.00	1.25	3.00	22.23	15.03
17	5.50	1.25	2.50	23.22	15.44

S – kimpul starch; CMF – cellulose microfiber; Gly – glycerol; TS – tensile strength; EAB – elongation at break.

Table 3: ANOVA for the quadratic response surface models.

Parameters	TS (MPa)	EAB (%)
Lack of fit	3.63	0.6838
R^2	0.9832	0.8608
Adjusted R^2	0.9617	0.6818
F-Value	45.63	4.81
Prob > F	<0.0001	0.0252
Press	144.33	62.26

TS – tensile strength; EAB – elongation at break.

EAB was primarily influenced by the linear and quadratic effects of CMF (B, B^2) and starch (A^2). The regression model yielded an F–value of 4.81 with a probability of 0.0252, confirming significance. However, the adjusted R^2 (0.6818) was lower than that for TS, indicating greater variability in EAB responses. This lower R^2 can be attributed to the inherently complex and sensitive nature of elongation at break, which depends on multiple competing factors, including filler–matrix interactions, plasticizer distribution, and microstructural heterogeneity. Slight variations in sample preparation, film thickness, or local inhomogeneities can disproportionately affect EAB measurements, thereby increasing experimental scatter.

As shown in Figure 1(B), EAB increased at moderate starch and glycerol levels but decreased when CMF exceeded 1.25%. This trend reflects a reinforcement–plasticizer balance: while TOCMF enhances stiffness and tensile strength, excessive loading restricts polymer chain mobility, thereby reducing extensibility. Conversely, glycerol enhances chain mobility, thereby increasing elongation; however, over–plasticization can compromise tensile integrity, highlighting the trade–off between strength and flexibility. Overall, despite the moderate R^2, the model remains valid for identifying general trends and optimizing composite formulations, though predictions for EAB should be interpreted with slightly greater caution than for TS.

The RSM results confirmed that starch, CMF, and glycerol exerted significant and interactive effects on the mechanical properties of the films. The highest tensile strength and modulus were obtained at relatively high starch and CMF loadings with moderate glycerol levels, whereas elongation was maximized under balanced conditions. These findings clearly demonstrate the effectiveness of TOCMF as a reinforcing filler and highlight its potential for the rational design of starch–based films with tailored performance for sustainable packaging applications.

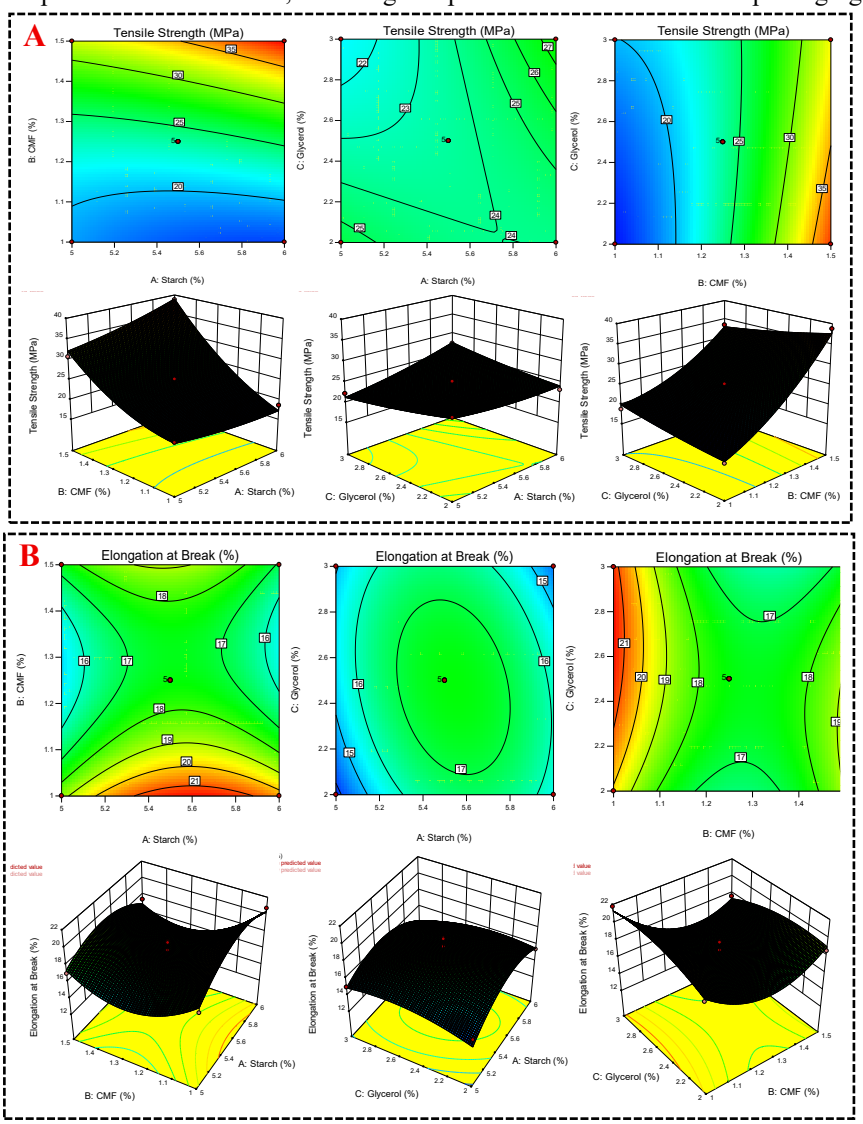

Figure 1: Response surface plots showing the effects of starch, CMF, and glycerol on (A) TS and (B) EAB of starch composite films.

3.2 *Particle size analysis of TOCMF and mechanical properties of films*

The SEM analysis of TOCMF and particle size analysis (Figure 2A–B) revealed that TOCMF had an average diameter of 2.685 µm, with most particles ranging from 1–4 µm. This size lies at the lower end of typical cellulose microfibers (5–50 µm) [26], [27] and is notably larger than cellulose nanofibers, which generally form only after additional high–energy mechanical treatments such as homogenization or ultrasonication [28], [29]. Because such post–oxidation disintegration was intentionally omitted, the TOCMF retained its micron-scale dimensions—an advantage that reduces energy demand and enhances process sustainability.

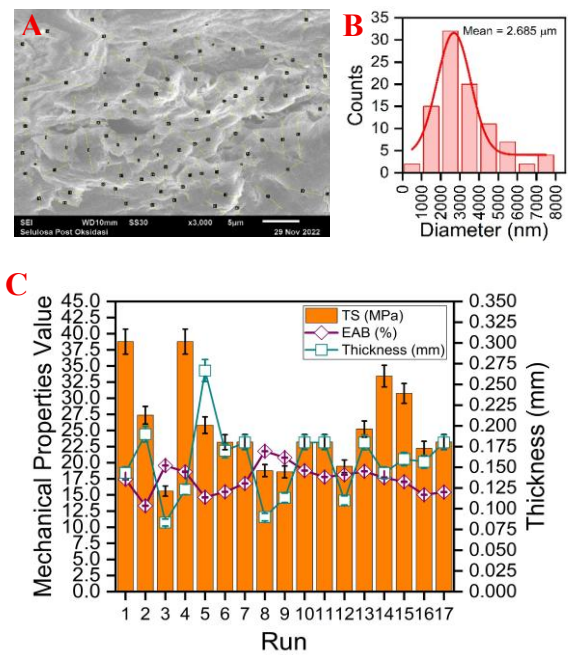

Figure 2: (A) SEM image and (B) particle size distribution of TOCMF and (C) TS, EAB, and film thickness of starch composite film.

Although it does not reach the nanoscale, micron-sized cellulose can still serve as an effective reinforcing filler due to its high aspect ratio and reactive surface groups [30]. Furthermore, bacterial cellulose from nata de coco is known for strong re–agglomeration tendencies, making nanofiber formation difficult without intensive mechanical disruption [31]. This intrinsic characteristic explains why the TEMPO–oxidized fibers in this study remained in the micro–scale range while still providing meaningful reinforcement. The results are consistent with prior findings that TEMPO oxidation introduces carboxylate groups at the C6 position, improving cellulose fibril dispersibility and hydrophilicity. This surface modification enhances interfacial compatibility in hydrophilic matrices such as kimpul starch films.

Previous studies have demonstrated that micro–fibrillated cellulose can significantly improve the strength and barrier properties of starch films through hydrogen bonding [20], and that micron–scale cellulose from agricultural residues can still serve as an effective reinforcing filler due to its high aspect ratio and surface functionality [21]. Thus, the TOCMF diameter of 2.685 µm is reasonable, without further fibrillation, and offers advantages in terms of reinforcement efficiency, energy savings, and processability.

Figure 2(C) shows that TS varied widely (15.60–38.78 MPa), with the highest values observed in formulations containing higher starch and 1.5% TOCMF (run 1 and run 4). The sharp reduction in TS at low starch/TOCMF (run 3) indicates that well–dispersed TOCMF is crucial for stress transfer in the polymer matrix, consistent with earlier reports where cellulose nanofibers enhanced TS through dense hydrogen–bonding networks [32].

EAB ranged from 13.33% to 21.78%, showing the typical inverse relation with TS. High TS films, such as run 4, displayed moderate elongation, while low–TS films showed greater ductility. This reflects a strengthening mechanism where increased TOCMF–starch hydrogen bonding restricts chain mobility, mirroring trends observed in other cellulose–reinforced starch composites [32]. The observed TS–EAB trade–off has direct implications for potential packaging applications: films with higher TS and moderate EAB are suitable for rigid packaging that requires structural integrity, whereas formulations with lower TS and higher elongation may be better suited for flexible or stretchable packaging.

Further, film thickness (0.09–0.26 mm) also influenced performance. Thinner films with more uniform TOCMF dispersion (e.g., run 4) yielded higher TS, whereas thicker films tended to exhibit lower TS due to greater risks of filler agglomeration and pore formation [33]. This highlights that microstructural homogeneity, rather than thickness alone, governs mechanical strength. Overall, the formulation of 5.5% starch + 1.5% TOCMF + 2.0%

glycerol (run 4) delivered the most balanced performance—with high TS (38.78 MPa), moderate EAB (18.59%), and low thickness (0.123 mm)—and was therefore selected as the optimal film for further characterization.

Table 4: Comparison of mechanical properties between the present study and starch–based films reinforced with fillers reported in previous studies.

Starch Matrices	Filler	TS (MPa)	EAB (%)	Ref.
Jackfruit seed	OPEFB and CMC	5.44	13.54	[19]
Cassava	MCC	16.70	1.31	[20]
Cassava	Banana bunch cellulose	6.72	4.02	[21]
Corn starch	Calcium carbonate	6.08	ND	[34]
Cassava peel	Cellulose PVA ZnO	37.38	ND	[14]
Corn cob	CMC	6.50	12.12	[35]
Kepok banana corm	Cellulose	5.92	8.00	[36]
Corn starch	Quercetin–loaded nanogel and CNC	14.2	8.8	[37]
Kimpul starch	TOCMF	38.78	18.59	This work

OPEFB–oil palm empty fruit bunch; CMC– carboxymethyl cellulose; MCC–microcrystalline cellulose; PVA–polyvinyl alcohol; Zinc oxide; TOCMF–TEMPO oxidation cellulose microfiber; TS –tensile strength; EAB–elongation at break; ND–no data.

The mechanical performance of starch–based films reinforced with various fillers reported in previous studies is also summarized in Table 4 for comparison. As shown, the TS of starch composites reported in earlier works generally ranged from 5.44 MPa to 37.38 MPa. For example, films derived from jackfruit seed starch reinforced with OPEFB and CMC exhibited a relatively low TS of 5.44 MPa [19]. Similarly, cassava starch reinforced with banana bunch cellulose reached only 6.72 MPa [21], while corn starch filler with calcium carbonate displayed 6.08 MPa [34]. Even though cassava peel starch reinforced with cellulose, PVA, and ZnO achieved a relatively higher TS of 37.38 MPa [14], its limitation lies in the use of multiple fillers, which increases complexity and production costs.

Compared to those conventional fillers, TOCMF provides superior reinforcement because TEMPO oxidation introduces abundant surface carboxyl groups on the cellulose fibers. These negatively charged $–COO^-$ groups enhance compatibility with starch by forming strong hydrogen bonds and electrostatic interactions with hydroxyl groups in the starch matrix, as supported by FTIR characterization shown in Figure 3. In contrast, MCC and untreated natural fibers possess fewer accessible functional groups and lower surface reactivity, resulting in weaker interfacial adhesion and less efficient stress transfer. The higher surface area and more individualized fibril structure of TOCMF further promote uniform dispersion, minimizing agglomeration and microvoids that typically weaken mechanical performance in MCC– or fiber–reinforced films. These interfacial advantages explain why TOCMF–containing composites in this study achieved significantly higher tensile strength despite using lower filler loading and simpler processing.

The present study demonstrated a substantial enhancement in the mechanical performance of starch–based films. The kimpul starch–TOCMF composite achieved a tensile strength of 38.78 MPa—exceeding nearly all previously reported starch films—while maintaining an EAB of 18.59%, which is distinctly higher than the commonly reported values below 14% [19], [35], [36] (Table 4). Achieving both high strength and high ductility simultaneously is rare in starch–based materials, highlighting the unique reinforcing capability of TOCMF.

Notably, the mechanical properties achieved in this work surpass those reported by Al–Naymi *et al.,* [37], whose prepared corn starch/hydroxypropyl methylcellulose film reinforced with CNC and quercetin–loaded nanogels reached a tensile strength of 14.2 MPa with an EAB of 8.8%. In contrast, the TOCMF–reinforced films in the present study exhibit more than double the tensile strength while maintaining substantially higher ductility, demonstrating a superior balance between strength and flexibility. These findings highlight the markedly stronger reinforcing capability of TOCMF, indicating that our starch-based composite outperforms CNC–based starch films in mechanical performance.

The superior balance between strength and flexibility indicates a synergistic reinforcement mechanism, where TOCMF facilitates efficient stress transfer and restricts polymer mobility without compromising extensibility. This dual enhancement underscores the novelty of the system and its strong potential for high–performance, sustainable packaging applications.

To clarify the structure–property relationship, complementary characterizations—including FTIR, XRD, thermal analysis, and SEM—were performed. These analyses collectively reveal how TOCMF modifies molecular interactions, crystallinity, and microstructure, ultimately contributing to the exceptional mechanical behavior of the composite films.

3.3 *FTIR analysis*

The FTIR spectra (Figure 3) revealed that the reinforcement of TOCMF led to a broadening and slight shift of the O–H stretching band toward lower wavenumbers compared with the starch–glycerol film (from 3428 to 3414 cm^{-1}). This phenomenon is consistent with hydrogen-bonding interactions between starch and cellulose fibers, as widely reported in similar studies. Poljaček *et al.,* observed that the O–H band of starch–nanocellulose films shifted from around 3300 cm^{-1} to 3250 cm^{-1}, indicating enhanced interfacial hydrogen bonding [38]. A similar trend was observed in the present study, which contributed to matrix reinforcement and consequently a relatively high TS.

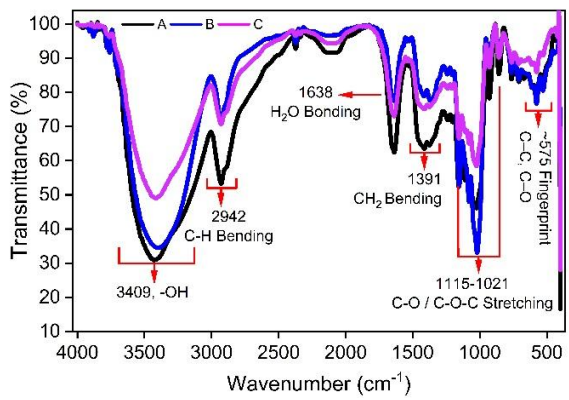

Figure 3: FTIR spectra of starch film (black), starch–glycerol film (blue), and optimized starch composite film (purple).

In addition, the increased intensity in the 1100–1020 cm^{-1} region indicated the contribution of C–O and C–O–C stretching from TOCMF. This result agrees with [39], who reported that MCC increased signals in this region due to improved ordering of glycosidic linkages. Implicitly, forming more intermolecular hydrogen bonds resulted in a denser polymer network, restricting starch chain mobility. FTIR thus not only confirmed the incorporation of TOCMF into the matrix and clarified the molecular mechanism supporting the mechanical results: stronger hydrogen bonding translates into improved TS.

3.4 *X–ray diffraction analysis*

The XRD patterns (Figure 4**)** further demonstrated that the CrI increased from 57.23% to 63.75% after TOCMF addition. This increase indicates that TOCMF acted as a nucleating agent, promoting starch chain orientation and tighter molecular packing. This trend is consistent with [40], who found that micro–fibrillated cellulose increased the CrI of starch films from 80 to 85%, accompanied by an increase in TS. The implications are clear: higher CrI reduces the free volume available for water molecule penetration, leading to denser, stiffer films with superior mechanical resistance.

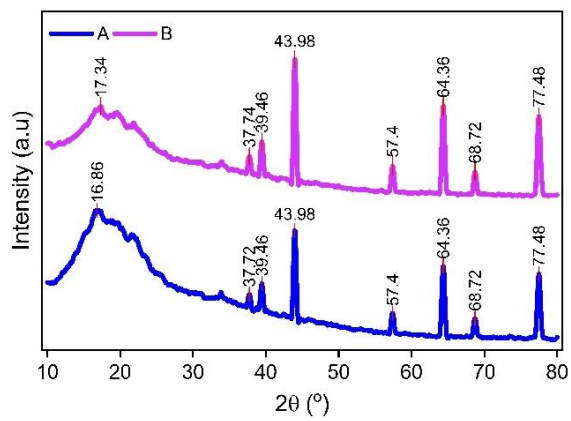

Figure 4: XRD patterns of starch–glycerol film (blue) and optimized starch composite film (purple).

The present study achieved a higher CrI than our previous reports [24], which may explain our films' greater TS values relative to similar studies (Table 4). Moreover, the increased CrI also correlated with improved barrier properties (SP, WL, MR, Figure 8), since higher semi–crystalline ordering hinders water diffusion. This mechanism reinforces the interpretation that TOCMF functions as a mechanical filler and a structural modifier that improves the internal ordering of starch–based films.

A more detailed examination of the XRD profiles was performed by assigning the characteristic diffraction peaks of A-type starch. Peaks at 2θ ≈ 15 °, 17°, 18°, and 23° correspond to the (110), (200), (020), and (210) planes, respectively, consistent with

previous reports [41]. These reflections became sharper and more intense after TOCMF addition, indicating enhanced structural ordering. Although crystallite size is commonly calculated using the Scherrer equation, this study focused on relative crystallinity changes and peak evolution because the primary objective was to evaluate the structural modification of starch matrices rather than to quantify absolute crystal dimensions. Similar qualitative interpretations have been adopted in a previous starch–cellulose composite study [24].

3.5 *Thermal analysis*

The thermal stability of the films was assessed using TGA, DTG, and DTA (Figure 5A–C; Table 5). All samples showed the typical multi-step degradation behavior of starch–based polymers. In the first stage (<200 °C), a minor mass loss of 12.1–17.4% occurred, corresponding to evaporation of bound water and low–molecular volatiles—consistent with previous reports on hydrophilic starch systems [42], [43]. The slightly lower moisture loss in the starch–glycerol film suggests stronger temporary hydrogen bonding between glycerol and starch that retains more water.

Major degradation took place between 200–350 °C due to glycosidic bond cleavage and starch depolymerization. Both the starch–glycerol and composite films degraded earlier than neat starch, reflecting the destabilizing effect of plasticization, which disrupts hydrogen bonding and increases chain mobility [44]. However, the composite film showed marginally higher thermal resistance than the starch–glycerol sample, indicating that CMF partially counteracts glycerol's destabilization through improved interfacial bonding.

Table 5: Thermal parameters of starch-based composite films obtained from TGA, DTG, and DTA analyses.

Samples	Initial weight loss (<200 °C, %)	Degradation (200–350 °C, %)	T_{max} (DTG peak, °C)	DTG_{max} (mg/min)	Residual mass (%)	DTA peak (μV)
Starch film (black)	12.4	76.0	310	0.708	24.0	−19.42
Starch–glycerol film (blue)	12.1	76.0	305	1.051	24.0	−21.07
Starch–glycerol–CMF composite film (purple)	17.4	74.2	308	0.788	25.8	−20.11

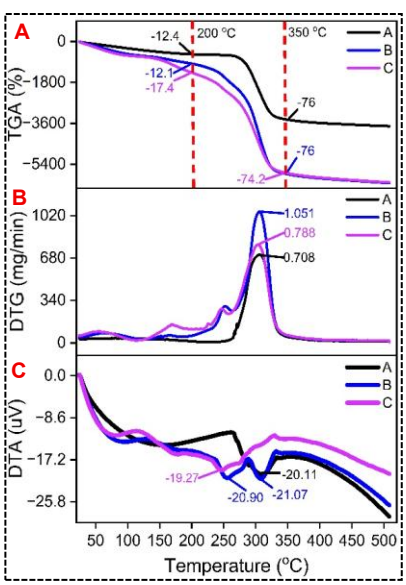

Figure 5: (A) TGA, (B) DTG, and (C) DTA curves of starch film (black), starch–glycerol film (blue), and optimized starch composite film (purple), respectively.

Importantly, the composite film produced a higher char yield (25.8%) compared to the other samples (24%). This suggests that CMF promotes dehydration and carbonization, forming a more stable protective layer during pyrolysis. Similar enhancements in char formation have been documented in starch–cellulose composites, where cellulose contributes to condensed–phase stabilization [45], [46].

The increased char residue indicates that the CMF–reinforced film maintains greater structural integrity at elevated temperatures, which is highly relevant for practical packaging operations. In industrial settings, biodegradable films must tolerate brief exposure to heat during processes such as heat sealing, thermal lamination, or hot–filling. The improved thermal stability observed in the CMF composite suggests greater resistance to thermal deformation, enabling more reliable sealing performance and reducing the risk of film shrinkage or rupture during processing. This improved residual stability highlights the reinforcing role of CMF and supports its potential for thermally robust, biodegradable packaging applications. This improved

residual stability highlights the reinforcing role of CMF and supports its potential for thermally robust, biodegradable packaging applications.

The DTG curves (Figure 5(B)) further confirmed these thermal trends. The neat starch film showed the lowest maximum degradation rate (0.708 mg/min), while the starch–glycerol film exhibited the highest (1.051 mg/min), indicating accelerated degradation due to weakened intermolecular cohesion. In contrast, the composite film degraded more slowly (0.788 mg/min), demonstrating that CMF restricts chain mobility and reinforces interfacial interactions. Similar reductions in degradation rate have been reported in starch–nanocellulose systems, where fibrillar fillers increase thermal tortuosity and delay volatile diffusion [47].

The DTA profiles (Figure 5(C)) showed endothermic transitions between 250–320 °C associated with chain scission and amorphous rearrangement. The neat starch film displayed a sharp transition, whereas the plasticized and composite films showed broader, lower–intensity peaks, reflecting structural heterogeneity induced by glycerol. Notably, the composite film exhibited a less negative endothermic signal (−20.11 μV) than the starch–glycerol film (−21.07 μV), consistent with the stabilizing effect of CMF, which redistributes thermal energy through an extended hydrogen–bonded network.

From an application standpoint, neat starch provides good thermal stability but is too brittle for practical packaging. Plasticization enhances flexibility but significantly lowers thermal resistance. The starch–glycerol–CMF composite offers the most balanced performance—combining flexibility, reinforced thermal stability, and superior mechanical strength. This synergy makes the composite suitable for food packaging processes involving heat sealing, drying, or mild pasteurization, where films must withstand thermal fluctuations. Overall, glycerol reduces thermal stability by increasing chain mobility, while CMF offsets this effect by strengthening the polymer network and reducing degradation kinetics, underscoring the composite film's promise as a thermally robust biodegradable packaging material.

3.6 *SEM morphology analysis*

The SEM images (Figure 6) illustrate clear morphological differences between the starch–glycerol film and the optimized TOCMF–reinforced composite. The starch–glycerol film (Figure 6A1–A2) shows a relatively smooth but discontinuous surface with microcracks, indicating poor compactness and weak interfacial bonding—features commonly linked to phase separation in plasticized starch systems and consistent with its lower tensile strength (18.78 MPa). Such surface discontinuities also facilitate moisture diffusion through the matrix, contributing to the weaker barrier performance observed in the grape storage test (Figure 8) [48].

In contrast, the composite film displays a denser and more uniform morphology (Figure 6(B1)–(B2)), with TOCMF well dispersed throughout the matrix and minimal agglomeration. The bright filler domains appear firmly integrated into the polymer network, suggesting adequate hydrogen bonding between TOCMF and starch chains, as supported by FTIR data (Figure 3). This improved interfacial adhesion reduces porosity, restricts chain mobility, and enhances stress transfer, contributing to the significantly higher tensile strength (38.78 MPa).

The compact microstructure also aligns with the increased crystallinity observed by XRD (63.75% vs. 57.23% in the starch–glycerol film; Figure 4), indicating that TOCMF acts as a nucleating agent and promotes ordered crystalline growth. Higher CrI generally correlates with reduced free volume and tighter molecular packing, which not only strengthens the film mechanically but also decreases water vapor transmission—supporting the superior barrier performance of the composite film. Such simultaneous improvements in compactness and crystallinity reflect a robust reinforcement mechanism typical of starch–cellulose composites [49], underscoring the effectiveness and novelty of TOCMF integration in the present system.

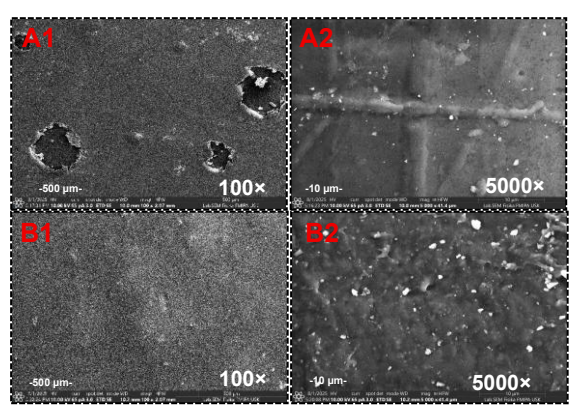

Figure 6: SEM images of (A1–A2) starch–glycerol film and (B1–B2) optimized starch composite film at 100 and 5000× magnification, respectively.

Previous studies have demonstrated that nanocellulose produced through high–pressure homogenization or ultrasonication provides strong reinforcement due to its high aspect ratio [50], [51]. However, the present results indicate that well–dispersed micron–scale TOCMF can deliver comparable improvements. This aligns with recent findings that TEMPO–oxidized microfibrils, despite their larger size, can enhance crystallinity and interfacial adhesion similarly to nanofibers because of their surface carboxylation [52]. Importantly, this avoids the energy–intensive nano–fibrillation step, offering a more sustainable and scalable route for industrial bioplastic production.

Poor filler dispersion is often associated with the formation of agglomerates and microvoids, which weaken mechanical performance. This behavior is evident in the starch–glycerol control film (Figure 6A), while the optimized composite shows a uniform TOCMF distribution with minimal defects. The resulting balanced properties—high tensile strength and modulus combined with moderate elongation—indicate that even a low TOCMF loading (1.5%) is sufficient to generate strong yet flexible films.

Moreover, the reduced porosity and better filler–matrix interlocking observed in the SEM images explain the lower swelling power (SP) and reduced moisture absorption of the composite film (Figure 8), which translated into significantly lower weight loss (WL) (3.51%) and higher mass retention (MR) (98.07%) in packaged grapes. This morphological–functional relationship confirms that microstructural improvements directly enhance the film's barrier properties.

Overall, the SEM observations confirm that nata–de–coco–derived TOCMF is an effective reinforcing agent for kimpul starch films. Its uniform dispersion, reduced porosity, and strong interfacial adhesion underpin the enhanced mechanical, structural, and barrier characteristics, "demonstrating how microstructural densification—supported by high CrI—translates into improved real-application performance during fruit storage." This shows that micron–scale TOCMF is a viable, energy–efficient alternative to conventional nanofibrils for the development of starch–based bioplastics.

3.7 *Composite film evaluations*

Figure 7 presents a visual comparison between the natural starch–glycerol film and the optimized starch composite film. The starch–glycerol film (Figure 7A) shows apparent morphological defects, including surface bubbles and micro–voids, along with visible cracks and a darker, non–uniform appearance. The presence of these voids indicates poor film–forming ability and heterogeneous polymer packing, which typically leads to increased brittleness and reduced structural cohesion. These morphological imperfections are consistent with the weak mechanical behavior of the neat starch–glycerol film, which was too brittle and rigid to be reliably tested for tensile properties. Films with such voids are prone to premature fracture and are unable to distribute stress effectively.

In contrast, the optimized composite film (Figure 7(B)) exhibits a smooth, uniform surface with no observable bubbles, cracks, or voids. The absence of these defects indicates improved intermolecular interactions and better compatibility between starch and TOCMF, resulting in more compact structural packing. This enhanced morphology aligns with the significantly improved mechanical performance of the composite film (Figure 2(C)), including higher tensile strength and elongation. The uniform microstructure facilitates more efficient stress transfer within the matrix, accounting for the composite film's superior flexibility and durability.

The effectiveness of both films in grape packaging is shown in Figure 7(C)–(F). At day 0, both materials produced transparent packaging. However, after 7 days, the starch–glycerol film (Figure 7(D)) exhibited moisture accumulation and reduced structural stability, indicating limited barrier performance. Conversely, grapes packaged with the composite film (Figure 7(F)) retained clearer, more stable packaging, demonstrating improved resistance to water vapor and gas permeability.

Quantitatively, grapes wrapped with the starch–glycerol film experienced a high weight loss (WL) of 20.364% and a mass retention (MR) of 79.636%. In contrast, the composite film significantly reduced WL to 3.51% and increased MR to 98.07%, confirming its superior protective capability. This performance is attributed to the denser polymer network formed by TOCMF reinforcement, which limits moisture diffusion more effectively than the hydrophilic starch–glycerol matrix (Figure 8). The high SP value of Sample A (116.619%) further reflects its strong water affinity, which accelerates moisture transfer and fruit dehydration, whereas Sample B exhibited a much lower SP (60.855%), indicating improved barrier behavior.

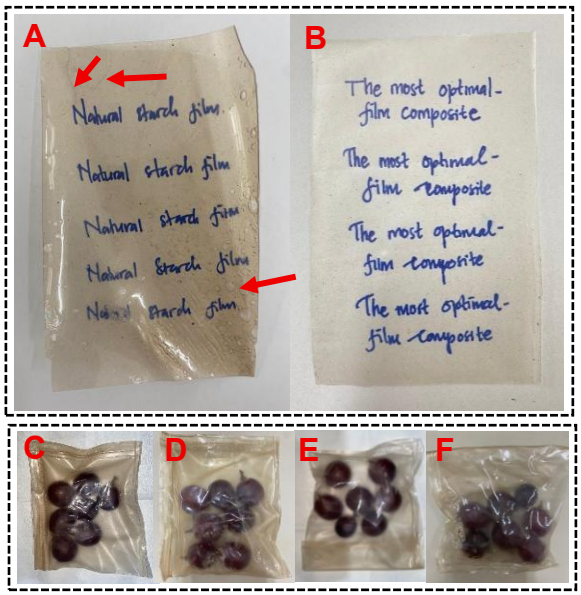

Figure 7: Photograph of (A) visual appearance of natural starch film; (B) the most optimal starch composite film; visual appearance of grapes packaged with (C, D) starch–glycerol film and (E, F) starch composite film at day 0 and day 7 of storage, respectively.

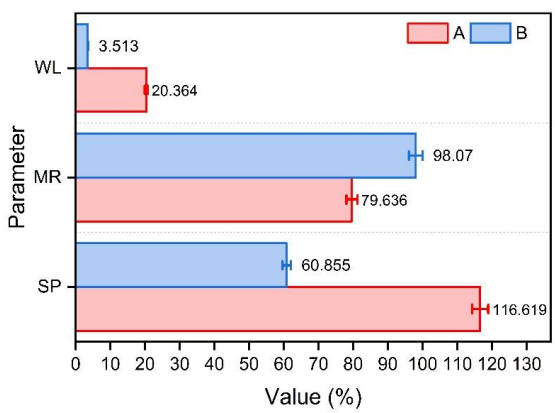

Figure 8: The SP of film, WL and MR of grapes wrapped with films after 7 days of storage. (A) starch–glycerol film (control) and (B) optimized starch composite film.

In practical terms, the significant difference in WL directly translates into meaningful shelf–life benefits. Grapes typically begin to show visible shrivelling when WL exceeds 5–7% [53]. With the control film already reaching >20% WL by day 7, the fruit is likely to pass its acceptable quality threshold within 3–4 days. By contrast, grapes wrapped with the composite film reached only 3.51% WL after 7 days, which is still below the shrivelling threshold. This suggests a potential shelf-life extension of approximately 2–3 days (a 40–60% increase) under similar storage conditions. Such an extension is highly relevant for transport and retail, where even a 1–2–day increase in firmness retention significantly reduces postharvest losses.

These observations align with previous findings that cellulose–based fillers enhance film compactness and water vapor resistance in starch composites, thereby reducing weight loss in packaged produce [20]. Maintaining high MR is critical for preserving grape freshness and sensory quality. Accordingly, the TOCMF–reinforced kimpul starch film demonstrates strong potential as an eco-friendly packaging material for extending the shelf life of grapes. Future improvements may include incorporating antimicrobial additives to further enhance protection and reduce storage losses.

It is important to note that grapes serve only as a model system to illustrate the film's protective performance under high–moisture conditions typical of fresh produce. The film's behavior may vary with product type, storage environment, and moisture content. Nevertheless, the enhanced barrier and mechanical properties of the TOCMF–reinforced film suggest broader potential applications, including packaging for other fresh produce with moderate respiration rates (e.g., tomatoes, strawberries), as well as dry or semi–dry foods (e.g., biscuits, spices, instant powders) that require moisture protection. Further studies involving different commodities and storage conditions will be necessary to fully validate the film's versatility in real–world food packaging scenarios.

4 Conclusions

This study demonstrated that incorporating TEMPO-oxidized cellulose microfibrils (TOCMF) into kimpul starch films markedly improved their mechanical, structural, and barrier properties. Response surface methodology (RSM) confirmed that starch, TOCMF, and glycerol exert significant and interactive effects on tensile strength, and elongation at break. The optimized formulation achieved a superior balance of strength and flexibility, with tensile strength values surpassing those reported for comparable starch-based composite films. These findings highlight the dual function of TOCMF as both a mechanical and structural modifier, enabling the development of starch-based composite films with enhanced integrity,

thermal stability, and barrier performance. The present work not only expands the utilization potential of underused kimpul starch but also provides valuable insights into the design of sustainable, high-performance biopolymer packaging materials.

Future work should explore the long-term stability, biodegradation behavior, and migration characteristics of the composite films under real packaging conditions. Further research could also evaluate scalability, cost analysis, and the integration of functional additives—such as antimicrobial or antioxidant agents—to broaden the prospects for application. Additionally, investigating the performance of TOCMF–starch films in multilayer or hybrid packaging systems may offer new opportunities for commercialization and industrial adoption.

Acknowledgements

The authors would like to thank the Institute for Research and Community Service (LPPM) Universitas Serambi Mekkah and the Ministry of Higher Education, Science and Technology of the Republic of Indonesia, with the scheme Beginner Lecturer Research (Penelitian Dosen Pemula) Grant Number: 134/C3/DT.05.00/PL/2025.

Author Contributions

F.H.: research design, data analysis, conceptualization, funding acquisition, investigation, reviewing and editing; A.N.: investigation, methodology, project administration; R.R. and E.I.: Validation, writing—reviewing and editing; S.N.: Software, reviewing and editing. A.A.K.: Investigation, visualization, writing an original draft, reviewing and editing. All authors have read and agreed to the published version of the manuscript.

Conflict of Interest

The authors declare no conflict of interest.

References

[1] S. S. Ali et al., "Microplastics as persistent and vectors of other threats in the marine environment: Toxicological impacts, management and strategical roadmap to end plastic pollution," *Environmental Chemistry and Ecotoxicology*, vol. 7, pp. 229–251, 2025, doi: 10.1016/j.enceco.2024.12.005.

[2] X. Zhao et al., "Sustainable bioplastics derived from renewable natural resources for food packaging," *Matter*, vol. 6, no. 1, pp. 97–127, Jan. 2023, doi: 10.1016/j.matt.2022.11.006.

[3] Yulianto, Julinawati, H. Fathana, and Rahmi, "Fabrication and characterization of chitosan film incorporated with ZnO and patchouli oil for food packaging," *International Journal of Design & Nature and Ecodynamics*, vol. 18, no. 5, pp. 1189–1194, Oct. 2023, doi: 10.18280/ijdne.180520.

[4] A. A. Kacaribu, R. Rahmi, J. Julinawati, H. Fathana, M. Reza, and M. Iqhramullah, "Preparation and characterization of cellulose film from velvet tamarind rind (*Dialium indum* L.) for food packaging," *Applied Science and Engineering Progress*, vol. 18, no. 3, Sep. 2025, Art. no. 7724, doi: 10.14416/j.asep.2025.03.006.

[5] A. A. Kacaribu and D. Darwin, "Biotechnological lactic acid production from low-cost renewable sources via anaerobic microbial processes," *BioTechnologia*, vol. 105, no. 2, pp. 179–194, 2024, doi: 10.5114/bta.2024.139757.

[6] S. Phongtamrug, P. Pilasen, and K. Ridthitid, "Effects of silane coupling agents on physical properties of simultaneous biaxially stretched polylactide film," *Applied Science and Engineering Progress*, vol. 17, no. 3, Jul. 2024, Art. no. 7406, doi: 10.14416/j.asep.2024.06.012.

[7] S. Phongtamrug, R. Makhon, and T. Wiriyosuttikul, "Enhanced performance of polylactide film via simultaneous biaxial stretching and silane coupling agent as a thermal shrinkable film," *Applied Science and Engineering Progress*, vol. 16, no. 2, Apr. 2023, Art. no. 5699, doi: 10.14416/j.asep.2022.02.008.

[8] H. Xue, L. Ji, K. Zhang, P. Wang, X. Liao, and J. Tan, "Preparation, properties, and applications of polysaccharide-based films: A comprehensive overview," *Journal of Future Foods*, pp. 1–114, doi: 10.1016/j.jfutfo.2025.05.011.

[9] T. R. Arruda et al., "An overview of starch-based materials for sustainable food packaging: Recent advances, limitations, and perspectives," *Macromolecules,* vol. 5, no. 2, Apr. 2025, Art. no. 19, doi: 10.3390/macromol5020019.

[10] K. Dhalsamant, A. Dalai, F. Pattnaik, and B. Acharya, "Biodegradable carbohydrate-based

films for packaging agricultural products—A review," *Polymers (Basel)*, vol. 17, no. 10, May 2025, Art. no. 1325, doi: 10.3390/polym17101325.

[11] S. A. Siddiqui, X. Yang, R. K. Deshmukh, K. K. Gaikwad, N. A. Bahmid, and R. Castro-Muñoz, "Recent advances in reinforced bioplastics for food packaging – A critical review," *International Journal of Biological Macromolecules*, vol. 263, Dec. 2023, Art. no. 130399, 2024, doi: 10.1016/j.ijbiomac.2024.130399.

[12] P. A. Pawase, et al., "Physical, chemical, and nano-enabled modifications of starch for sustainable food packaging films: Recent trends, challenges, and prospects," *Carbohydrate Polymers: Technology and Applications*, Aug. 2025, Art. no. 100986, doi: 10.1016/j.carpta.2025.100986.

[13] E. C. Emenike, K. O. Iwuozor, O. D. Saliu, J. Ramontja, and A. G. Adeniyi, "Advances in the extraction, classification, modification, emerging and advanced applications of crystalline cellulose: A review," *Carbohydrate Polymers: Technology and Applications*, vol. 6, Jun. 2023, Art. no. 100337, doi: 10.1016/j.carpta.2023.100337.

[14] Hendrawati, A. R. Liandi, H. Ahyar, I. Maladi, A. Azhari, and M. Cornelia, "The influence of the filler addition of rice husk cellulose, polyvinyl alcohol, and zinc oxide on the characteristics of environmentally friendly cassava biodegradable plastic," *Case Studies in Chemical and Environmental Engineering*, vol. 8, Aug. 2023, Art. no. 100520, doi: 10.1016/j.cscee.2023.100520.

[15] Z. Wang, S. Li, X. Zhao, Z. Liu, R. Shi, and M. Hao, "Applications of bacterial cellulose in the food industry and its health-promoting potential," *Food Chemistry*, vol. 464, no. P2, Feb. 2025, Art. no. 141763, doi: 10.1016/j.foodchem.2024.141763.

[16] F. Zhu, "Starch based films and coatings for food packaging: Interactions with phenolic compounds," *Food Research International*, vol. 204, Jan. 2025, Art. no. 115758, doi: 10.1016/j.foodres.2025.115758.

[17] S. Fatima, M. R. Khan, I. Ahmad, and M. B. Sadiq, "Recent advances in modified starch based biodegradable food packaging: A review," *Heliyon*, vol. 10, no. 6, Mar. 2024, Art. no. e27453, doi: 10.1016/j.heliyon.2024.e27453.

[18] F. S. Rejeki, D. Puspitasari, and E. R. Wedowati, "Kimpul (*Xanthosoma sagitifolium*) liquid sugar with low glycemic index," *Food Science and Applied Biotechnology*, vol. 3, no. 2, Oct. 2020, Art. no. 185, doi: 10.30721/fsab2020.v3.i2.84.

[19] N. Sasria, V. N. Afifah, G. Umindya, and N. Tajalla, "Effect of sorbitol plasticizer on bioplastics properties based on oil palm empty fruit bunches (OPEFB) and jackfruit seed starch," *Makara Journal of Science*, vol. 29, no. 2, 2025, doi: 10.7454/mss.v29i2.2192.

[20] A. H. D. Abdullah, O. D. Putri, A. K. Fikriyyah, R. C. Nissa, and S. Intadiana, "Effect of microcrystalline cellulose on characteristics of cassava starch-based bioplastic," *Polymer Testing and Materials*, vol. 59, no. 12, pp. 1250–1258, Aug. 2020, doi: 10.1080/25740881.2020.1738465.

[21] C. A. Saputri, F. A. Julyatmojo, Harmiansyah, M. Febrina, M. Mahardika, and S. Maulana, "Characteristics of bioplastics prepared from cassava starch reinforced with banana bunch cellulose at various concentrations," *IOP Conference Series: Earth and Environmental Science*, vol. 1309, no. 1, Mar. 2024, Art. no. 012006, doi: 10.1088/1755-1315/1309/1/012006.

[22] Z. Tang et al., "TEMPO-oxidized cellulose with high degree of oxidation," *Polymers*, vol. 9, no. 9, pp. 3–4, 2017, doi: 10.3390/polym9090421.

[23] C. Mouro, A. Gomes, and A. P. Gomes, "Sustainable bacterial cellulose production using low-cost fruit wastewater feedstocks," *Nanomaterials*, vol. 15, no. 271, pp. 1–26, 2025, doi: 10.3390/nano15040271.

[24] F. Hidayat, E. Indarti, Rahmi, and N. Arahman, "Synthesis of a biocomposite based on Kluwih (*Artocarpus camansi*) seed starch incorporated with carrageenan as a functional additive and cellulose nanofiber filler," *Case Studies in Chemical and Environmental Engineering*, vol. 11, Jun. 2025, Art. no. 101120, doi: 10.1016/j.cscee.2025.101120.

[25] L. Segal, J. J. Creely, A. E. Martin, and C. M. Conrad, "An empirical method for estimating the degree of crystallinity of native cellulose using the X-ray diffractometer," *Textile Research Journal*, vol. 29, no. 10, pp. 786–794, 1959, doi: 10.1177/004051755902901003.

[26] H. Khalili et al., "Starch biocomposites based on cellulose microfibers and nanocrystals extracted from alfa fibers (*Stipa tenacissima*),"

International Journal of Biological Macromolecules, vol. 226, pp. 345–356, Jan. 2023, doi: 10.1016/j.ijbiomac.2022.11.313.

[27] T. A. Do, V. Q. Nguyen, T. M. C. Nguyen, T. H. N. Nguyen, and T. H. Le, "A one-step chemical treatment to directly isolate microcrystalline cellulose from lignocellulose source," *Bioresources and Bioprocessing*, vol. 12, no. 1, Aug. 2025, Art. no. 89, doi: 10.1186/s40643-025-00920-6.

[28] X. Cao, B. Ding, J. Yu, and S. S. Al-Deyab, "Cellulose nanowhiskers extracted from TEMPO-oxidized jute fibers," *Carbohydrate Polymers*, vol. 90, no. 2, pp. 1075–1080, Oct. 2012, doi: 10.1016/j.carbpol.2012.06.046.

[29] J. Park, et al., "Effect of catalyst and oxidant concentrations in a TEMPO oxidation system on the production of cellulose nanofibers," *RSC Advances*, vol. 14, no. 45, pp. 32852–32862, 2024, doi: 10.1039/D4RA04948A.

[30] M. D. Panaitescu, A. Nicoleta, M. Ghiurea, C. Ilie, C. Radovici, and M. Doina, "Properties of polymer composites with cellulose microfibrils," in *Advances in Composite Materials: Ecodesign and Analysis*, InTech, March 2011, doi: 10.5772/14682.

[31] T. A. Nguyen and X. C. Nguyen, "Bacterial cellulose-based biofilm forming agent extracted from Vietnamese nata-de-coco tree by ultrasonic vibration method: Structure and properties," *Journal of Chemistry*, vol. 2022, pp. 1–10, Aug. 2022, doi: 10.1155/2022/7502796.

[32] C. Zhang, S. S. Nair, H. Chen, N. Yan, R. Farnood, and F. Li, "Thermally stable, enhanced water barrier, high strength starch bio-composite reinforced with lignin containing cellulose nanofibrils," *Carbohydrate Polymers*, vol. 230, Feb. 2020, Art. no. 115626, doi: 10.1016/j.carbpol.2019.115626.

[33] A. Jansson and F. Thuvander, "Influence of thickness on the mechanical properties for starch films," *Carbohydrate Polymers*, vol. 56, no. 4, pp. 499–503, Jul. 2004, doi: 10.1016/j.carbpol.2004.03.019.

[34] M. K. Gurunathan, R. J. H. Navasingh, J. D. R. Selvam, and R. Čep, "Development and characterization of starch bioplastics as a sustainable alternative for packaging," *Scientific Reports*, vol. 15, no. 1, May 2025, Art. no. 15264, doi: 10.1038/s41598-025-00221-0.

[35] M. B. Ihsan and Ratnawulan, "Effect of carboxymethyl cellulose (CMC) addition on the quality of biodegradable plastic from corn cob," *Jurnal Penelitian Pendidikan IPA*, vol. 9, no. 7, pp. 5117–5125, Jul. 2023, doi: 10.29303/jppipa.v9i7.4010.

[36] H. Nasution, B. H. Manurung, and N. Nofifah, "Effect of glycerol concentration and filler addition on the properties of bioplastics derived from Kepok banana corm starch," *Jurnal Rekayasa Kimia dan Lingkungan*, vol. 20, no. 1, pp. 196–207, 2025, doi: 10.23955/rkl.v20i1.42461.

[37] H. A. S. Al-Naymi et al., "Development of an innovative reinforced food packaging film based on corn starch/hydroxypropyl methylcellulose/ nanocrystalline cellulose incorporated with nanogel containing quercetin," *Food and Bioprocess Technology*, vol. 18, pp. 1514–1533, 2025, doi: 10.1007/s11947-024-03545-3.

[38] S. M. Poljaček et al, "Starch-based functional films enhanced with bacterial nanocellulose for smart packaging: Physicochemical properties, pH sensitivity and colorimetric response," *Polymers*, vol. 16, no. 16, Aug. 2024. Art. no. 2259, doi: 10.3390/polym16162259.

[39] J. Xiong, Q. Li, Z. Shi, and J. Ye, "Interactions between wheat starch and cellulose derivatives in short-term retrogradation: Rheology and FTIR study," *Food Research International*, vol. 100, pp. 858–863, 2017, doi: 10.1016/j.foodres.2017.07.061.

[40] M. M. González-Pérez, M. G. Lomelí-Ramírez, J. R. Robledo-Ortiz, J. A. Silva-Guzmán, and R. Manríquez-González, "Biodegradable biocomposite of starch films cross-linked with polyethylene glycol diglycidyl ether and reinforced by microfibrillated cellulose," *Polymers*, vol. 16, no. 9, May 2024, Art. no. 1290, doi: 10.3390/polym16091290.

[41] Y. Liu, H. Xie, and M. Shi, "Effect of ethanol–water solution on the crystallization of short chain amylose from potato starch," *Starch/Stärke*, vol. 68, no. 7–8, pp. 683–690, 2016, doi: 10.1002/star.201500300.

[42] X. He et al., "Effect of starch plasticization on morphological, mechanical, crystalline, thermal, and optical behavior of poly(butylene adipate-co-terephthalate)/thermoplastic starch composite films," *Polymers*, vol. 16, no. 3, Jan. 2024, Art. no. 326, doi: 10.3390/polym16030326.

[43] N. Nordin, S. H. Othman, S. A. Rashid, and R. K.

Basha, "Effects of glycerol and thymol on physical, mechanical, and thermal properties of corn starch films," *Food Hydrocolloids*, vol. 106, Sep. 2020, Art. no. 105884, doi: 10.1016/j.foodhyd.2020.105884.

[44] V. Ciaramitaro et al., "From micro to macro: Physical-chemical characterization of wheat starch-based films modified with PEG200, sodium citrate, or citric acid," *International Journal of Biological Macromolecules*, vol. 253, no. P5, Dec. 2023, Art. no. 127225, doi: 10.1016/j.ijbiomac.2023.127225.

[45] M. Ahmadi, O. Zabihi, Z. K. Nia, V. Unnikrishnan, C. J. Barrow, and M. Naebe, "Engineering flame and mechanical properties of natural plant-based fibre biocomposites," *Advanced Industrial and Engineering Polymer Research*, vol. 8, no. 2, pp. 168–195, 2025, doi: 10.1016/j.aiepr.2024.08.002.

[46] H.-B. Yuan, R.-C. Tang, and C.-B. Yu, "Flame retardant functionalization of microcrystalline cellulose by phosphorylation reaction with phytic acid," *International Journal of Molecular Sciences*, vol. 22, no. 17, Sep. 2023, Art. no. 9631, doi: 10.3390/ijms22179631.

[47] S. P. Bangar and W. S. Whiteside, "Nano-cellulose reinforced starch biocomposite films — a review on green composites," *International Journal of Biological Macromolecules*, vol. 185, pp. 849–860. 2021, doi: 10.1016/j.ijbiomac.2021.07.017.

[48] S. Mao, F. Li, X. Zhou, C. Lu, and T. Zhang, "Characterization and sustained release study of starch-based films loaded with carvacrol: A promising UV-shielding and bioactive nanocomposite film," *LWT — Food Science and Technology*, vol. 180, Apr. 2023, Art. no. 114719, doi: 10.1016/j.lwt.2023.114719.

[49] M. O. Reis, J. Zanela, J. Olivato, P. S. Garcia, F. Yamashita, and M. V. E. Grossmann, "Microcrystalline cellulose as reinforcement in thermoplastic starch/poly(butylene adipate-co-terephthalate) films," *Journal of Polymers and the Environment*, vol. 22, no. 4, pp. 545–552, 2014, doi: 10.1007/s10924-014-0674-7.

[50] C. Negro et al., "Synergies between fibrillated nanocellulose and hot-pressing of papers obtained from high-yield pulp," *Nanomaterials*, vol. 13, no. 13. Jun. 2023, Art. no. 1931, doi: 10.3390/nano13131931.

[51] K. Zhang et al., "Preparation of cellulose nano/microfibres with ultra-high aspect ratios from tobacco stem using soda-oxygen delignification and ultrasonication," *Cellulose*, vol. 30, no. 9, pp. 5607–5622, 2023, doi: 10.1007/s10570-023-05215-7.

[52] Y. Okita, T. Saito, and A. Isogai, "Entire surface oxidation of various cellulose microfibrils by TEMPO-mediated oxidation," *Biomacromolecules*, vol. 11, no. 6, pp. 1696–1700, 2010, doi: 10.1021/bm100214b.

[53] V. Ramprasad, Y. N. Reddy, and M. G. D. M. Reddy, "Studies on extension of shelf-life of grape through antioxidants and alternative inhibitors," *Acta Horticulturae*, vol. 662, pp. 397–402, 2004, doi: 10.17660/ActaHortic.2004.662.60.